3-18-2016

Disc Outflows and High-Luminosity True Type 2 AGN

Moshe Elitzur
University of Kentucky, moshe@pa.uky.edu

Hagai Netzer
Tel Aviv University, Israel

Right click to open a feedback form in a new tab to let us know how this document benefits you.

Disc Outflows and High-Luminosity True Type 2 AGN

Disc outflows and high-luminosity true type 2 AGN

Moshe Elitzur[1,2]★ and Hagai Netzer[3]

[1]*Astronomy Department, University of California, Berkeley, CA 94720-3411, USA*
[2]*Department of Physics and Astronomy, University of Kentucky, Lexington, KY 40506-0055, USA*
[3]*School of Physics and Astronomy, Tel Aviv University, Tel Aviv 69978, Israel*

ABSTRACT

The absence of intrinsic broad-line emission has been reported in a number of active galactic nuclei (AGN), including some with high Eddington ratios. Such 'true type 2 AGN' are inherent to the disc-wind scenario for the broad-line region: broad-line emission requires a minimal column density, implying a minimal outflow rate and thus a minimal accretion rate. Here we perform a detailed analysis of the consequences of mass conservation in the process of accretion through a central disc. The resulting constraints on luminosity are consistent with all the cases where claimed detections of true type 2 AGN pass stringent criteria, and predict that intrinsic broad-line emission can disappear at luminosities as high as $\sim 4 \times 10^{46}$ erg s^{-1} and any Eddington ratio, though more detections can be expected at Eddington ratios below ~ 1 per cent. Our results are applicable to every disc outflow model, whatever its details and whether clumpy or smooth, irrespective of the wind structure and its underlying dynamics. While other factors, such as changes in spectral energy distribution or covering factor, can affect the intensities of broad emission lines, within this scenario they can only produce true type 2 AGN of higher luminosity then those prescribed by mass conservation.

Key words: galaxies: active – galaxies: nuclei – quasars: emission lines – quasars: general.

1 INTRODUCTION

Although active galactic nuclei (AGN) unification is supported by a large body of evidence, it is still incomplete in several ways. In the standard unification scenario, all AGN are intrinsically the same, except for their luminosity, and produce the same broad emission line spectrum. The only reason we do not observe the broad emission lines in type 2 AGN is our viewing angle with respect to the toroidal obscuration that surrounds the central engine (e.g. Antonucci 1993). However, the structure of the AGN environment must evolve with accretion rate and luminosity – obviously the AGN disappears altogether once the accretion rate drops to zero. The question is whether the evolution induced by the decline of accretion rate produces discernible effects before that final point is reached; that would imply that all AGN are in fact not intrinsically the same.

An increasing number of AGN are reportedly missing broad emission lines, or the lines are extremely weak, even though there is little or no obscuration to their central source. First noticed in low-luminosity AGN with low Eddington ratios (see, among others, Tran 2001, 2003; Panessa & Bassani 2002; Laor 2003), this phenomenon has now been reported also in high Eddington-ratio AGN (Ho, Kim & Terashima 2012; Miniutti et al. 2013). Since the first reported ob-

jects of this type show prominent narrow emission lines, they were referred to as 'true type 2 AGN'. However, the unusual appearance is related more to the strength of the broad emission lines relative to the non-stellar continuum, and the above name (which will be retained for the rest of the paper) will be used to describe AGN with weak broad emission lines, whatever the narrow-line strength.

Conclusively establishing the absence of emission features is always difficult. Indeed, Stern & Laor (2012a,b) have noted that the observed upper limits on broad Hα emission in some previously claimed true type 2 AGN are insufficient to establish decisively the true nature of these sources. This ambiguity does not mean that broad Hα must be there, only that the data are not yet conclusive in demonstrating its complete absence. Stern & Laor also noted that there are sources where the absence of broad Hα emission is established with such stringent upper limits, well below the level expected from their X-ray luminosities, that they indeed appear to be true type 2 AGN. Another serious difficulty is time variability. Some AGN, dubbed 'changing look quasars', display temporal variations in broad-line strengths that cannot be attributed to transient obscuration and must be related to a large sudden drop in accretion rate (see LaMassa et al. 2015; MacLeod et al. 2016, and references therein). While some of the suggested cases of true type 2 AGN undoubtedly reflect such temporary reductions in broad Hα strength, multi-epoch observations preclude this possibility in a number of others. On the basis of current observational evidence, here we

take the view that the true type 2 phenomenon merits additional serious considerations and seek a general theoretical framework to explain it.

Observations suggest that the broad-line region (BLR) and the toroidal obscuration region (TOR, a.k.a. 'the torus') may be the inner and outer zones, respectively, in a single, continuous distribution of material whose composition undergoes a change at the dust sublimation radius (see Elitzur 2008, and references therein). Such a structure arises naturally in the disc–wind scenario, where the source of material to the BLR and the TOR is mass outflow from the surface of a disc that extends to distances that are an order of magnitude larger than a 'typical' BLR size (measured by reverberation mapping to be $\sim 10^3$–10^4 gravitational radii). The immediate prediction of this scenario (Elitzur & Shlosman 2006) is that at low accretion rates, the mass outflow rate decreases too and the wind radial column density eventually drops below the minimum required to produce detectable broad-line emission in the dust-free zone and continuum obscuration in the dusty zone. In this scenario, true type 2 AGN inevitably emerge at low accretion rates.

Elitzur & Ho (2009) presented a preliminary analysis of mass conservation in the disc–wind scenario at low accretion rates. They argued that the disappearance of the BLR and TOR should occur at bolometric luminosities that obey $L \propto M^{2/3}$, where M is the black hole (BH) mass, with a proportionality coefficient that varies among sources. While that study focused on the low-luminosity end, here we present a more complete analysis and examine in detail whether mass conservation and the constraints it implies can also explain the reported high-luminosity true type 2 AGN.

2 CONSTRAINTS ON BROAD-LINE EMISSION

Detectable broad-line emission requires a minimal column density, $N_{\mathrm{H,min}}$, to produce radial stratification with photoionization and recombination events occurring at a sufficient rate. The fundamental quantity $N_{\mathrm{H,min}}$ that sets the threshold for detectable emission lines is determined by physical processes and atomic constants, and is largely independent of the AGN detailed structure. Following the results of detailed photoionization calculations (e.g. Netzer 2013), we adopt $N_{\mathrm{H,min}} = 5 \times 10^{21}$ cm^{-2}. Denote

$$N_{\mathrm{R}} = \int n(R)\mathrm{d}R \qquad (1)$$

the column density along a radial ray close to the AGN equatorial plane, where R is axial radius and n is the gas density. Since the column is expected to decrease, or at least not to increase, away from the equator towards the poles, no other radial column is larger than N_{R}. Therefore, to produce a BLR the column N_{R} must exceed $N_{\mathrm{H,min}}$, namely,

$$N_{\mathrm{R}} > N_{\mathrm{H,min}}. \qquad (2)$$

This is a fundamental constraint that must be obeyed by all broad-line emitting AGN. It involves no assumptions about the BLR detailed structure or dynamics.

2.1 Mass conservation constraint

While the column $N_{\mathrm{H,min}}$ is controlled by basic physical processes, N_{R} is a specific property of each AGN and cannot be calculated without some assumptions about the structure of its BLR. Here we invoke the disc–wind scenario for the BLR and derive N_{R} from mass continuity for the outflow.

In the disc–wind scenario, the BLR corresponds to a portion of the wind ejected from a finite annular segment of the disc whose outer radius is set by dust sublimation. Denote by $\dot{M}_{\mathrm{w}}$ the overall mass outflow rate from that segment of the disc. Accounting for emission from both faces of a disc,[1] the mass conservation relation for a smooth-density disc outflow is

$$\dot{M}_{\mathrm{w}} = 4\pi m_{\mathrm{p}} \int n v_z R \mathrm{d}R, \qquad (3)$$

where m_{p} is the proton mass, v_z is the outflow velocity vertical component at the disc surface and R and n as in equation (1). We now introduce characteristic scales for the variables. For R we use the dust sublimation radius R_{d} so that dimensionless distance from the axis is

$$y = \frac{R}{R_{\mathrm{d}}} \qquad (4)$$

and the origin of the BLR outflow corresponds to disc radii $y \leq 1$ (the TOR has $y \geq 1$). We write the launch velocity as $v_z(R) = v_{\mathrm{K}}(R)f(R)$, where $v_{\mathrm{K}}(R)$ is the local Keplerian velocity and $f(<1)$ a dimensionless profile, and introduce

$$v_{\mathrm{Kd}} = v_{\mathrm{K}}(R_{\mathrm{d}}) = \left(\frac{GM}{R_{\mathrm{d}}} \right)^{1/2}. \qquad (5)$$

Then the outflow launch velocity becomes

$$v_z(y) = v_{\mathrm{Kd}} \frac{f(y)}{y^{1/2}}. \qquad (6)$$

With N_{R} from equation 1, we extract from the density n its dimensionless radial profile η through

$$n(y) = \frac{N_{\mathrm{R}}}{R_{\mathrm{d}}} \eta(y), \qquad \text{so that} \quad \int \eta(y)\mathrm{d}y = 1. \qquad (7)$$

The profile η, normalized to unit integral, describes the functional form of the density radial variation, e.g. a power law, etc. (see Section 3.1 below). With these definitions, equation (3) becomes

$$\dot{M}_{\mathrm{w}} = 4\pi m_{\mathrm{p}} R_{\mathrm{d}} v_{\mathrm{Kd}} N_{\mathrm{R}} I, \qquad \text{where} \quad I = \int f\eta y^{1/2}\mathrm{d}y. \qquad (8)$$

This is the mass conservation relation in terms of the radial column N_{R} through the disc outflow. Inserting N_{R} from this result into equation (2) yields a constraint on the mass outflow rate in broad-line emitting AGN. This constraint can be cast in the convenient form

$$N_{\mathrm{w}} > I N_{\mathrm{H,min}}, \quad \text{where} \quad N_{\mathrm{w}} = \frac{\dot{M}_{\mathrm{w}}}{4\pi m_{\mathrm{p}} R_{\mathrm{d}} v_{\mathrm{Kd}}} \qquad (9)$$

is a characteristic column density formed out of the outflow parameters (see Elitzur, Ho & Trump 2014, which used the notation N_{crit} for this quantity). This is the BLR constraint (equation 2) in the disc–wind scenario, expressed in terms of global properties of the system. All detailed information about the specific structure of a given AGN, i.e. the functional forms of its density and velocity radial distribution profiles, is contained in a single factor, the dimensionless integral I.

A clumpy disc-outflow yields the exact same result. Denote by M_{c} the mass of a single cloud, v_{c} its vertical launch velocity and n_{c} the number density of clouds (number of clouds per unit volume). Integrating over the disc area then gives $\dot{M}_{\mathrm{w}} = 4\pi \int M_{\mathrm{c}} n_{\mathrm{c}} v_{\mathrm{c}} R \mathrm{d}R$. If $N_{\mathrm{H}}^{\mathrm{c}}$ is the column density of a single cloud and A_{c} its cross-sectional area then $M_{\mathrm{c}} = m_{\mathrm{p}} N_{\mathrm{H}}^{\mathrm{c}} A_{\mathrm{c}}$. Since $N_{\mathrm{c}} \equiv n_{\mathrm{c}} A_{\mathrm{c}}$ is the number

---

[1] Elitzur & Ho (2009) is missing a factor of 2 for emission from both sides.

of clouds per unit length, $\dot{M}_w = 4\pi m_p \int N_H^c N_c v_c\, R dR$. Denote by $\mathcal{N}_0 \equiv \int N_c\, dR$ the (mean of the) total number of clouds along a radial equatorial ray, then the total radial column at the base of the wind (just above the disc surface) is $N_R = \mathcal{N}_0 N_H^c$. Introducing $\eta = N_c(R) R_d / \mathcal{N}_0$ yields back equation (8) with the same definition of f; the only difference is that now η is the normalized radial distribution of the number of clouds per unit length instead of gas density. Given this, there is no need to distinguish between the smooth and clumpy components of the wind; N_R is the total radial column density of the outflow at its origin above the disc surface irrespective of clumpiness.

The constraint in equation (9) on broad-line emitting AGN is a fundamental property of the disc–wind scenario. As a direct consequence of mass conservation (equation 3), it is in essence a kinematic outcome of this scenario that does not involve any assumptions about the wind dynamics, and is applicable for both smooth and clumpy outflows.

2.2 Luminosity constraint

Equation (9) provides a general constraint on disc outflows in broad-line emitting AGN. Unfortunately, this relationship has limited direct utility since it involves the BLR mass outflow rate $\dot{M}_w$, which is not readily measurable. For comparison with observations, we wish to relate $\dot{M}_w$ to the bolometric luminosity L. BH mass accretion at the rate $\dot{M}$ generates the luminosity $L = \epsilon \dot{M} c^2$, where ϵ is the radiative conversion efficiency. Since we are interested in the mass outflow rate $\dot{M}_w$, we introduce the ratio $r = \dot{M}/\dot{M}_w$ so that

$$L = \epsilon r \dot{M}_w c^2. \tag{10}$$

In this variation on the standard luminosity relation, the BH mass accretion rate $\dot{M}$ is replaced by the BLR outflow rate $\dot{M}_w$, hence the radiative efficiency is replaced by the product ϵr. With this, equation (8) for the relation between $\dot{M}_w$ and N_R becomes

$$L = 4\pi m_p c^2\, \epsilon r I\, (GMR_d)^{1/2} N_R. \tag{11}$$

This is the relation between the AGN luminosity and the radial column density of the outflow at its origin above the disc. It is not yet in suitable form since the luminosity enters also indirectly on the right-hand side because of the L-dependence of dust sublimation. The dust sublimation radius obeys the relation $R_d = b\, L_{45}^{1/2}$ pc, where $L_{45} = L/10^{45}$ erg s^{-1} and b is a normalization factor that depends on the dust composition. Nenkova et al. (2008) considered a standard graphite-silicate dust mixture that yields $b = 0.43$. Mor & Netzer (2012) suggest that, since only pure graphite grains survive in the torus innermost part, $b \simeq 0.16$ should be used instead. This is in good agreement with the most recent dust reverberation results of Koshida et al. (2014), and thus is the value we adopt here. Then equation (11) becomes

$$N_R = \frac{2.07 \times 10^{21}}{\epsilon r I} \left(\frac{L_{45}}{M_7^{2/3}} \right)^{3/4} cm^{-2}, \tag{12}$$

where $M_7 = M/10^7\, M_\odot$. This is the final relation for radial column density in terms of mass and luminosity in all disc outflows. With it, the broad-line emission constraint $N_R > N_{H,min}$ (equation 2) becomes

$$L > L_{min}, \tag{13}$$

where

$$L_{min} = \Lambda M_7^{2/3}, \quad \text{and} \quad \Lambda = 3.25 \times 10^{45}\, (\epsilon r I)^{4/3}\, erg\, s^{-1}. \tag{14}$$

This is the minimal luminosity for the existence of an observable BLR in the disc–wind scenario (cf. Elitzur & Ho 2009). Objects whose luminosity falls below this limit do not have a visible BLR and are classified as true type 2 AGN. The relation between L_{min} and the Eddington luminosity, $L_{Edd} = 1.26 \times 10^{45} M_7$ erg s^{-1}, is

$$\frac{L_{min}}{L_{Edd}} = 2.58 \left[\frac{(\epsilon r I)^4}{M_7} \right]^{1/3}. \tag{15}$$

Systems with masses $M_7 < 17.2\, (\epsilon r I)^4$ will have $L_{Edd} < L_{min}$, thus they will necessarily be true type 2 AGN if they have sub-Eddington luminosities.

3 NUMERICAL ESTIMATES

Equation (13) provides the fundamental constraint on broad-line emission in the disc–wind scenario, imposing a lower limit on AGN luminosity that varies with the BH mass. Because each of the three parameters I, r and ϵ can vary from source to source, Λ is expected to vary among AGN (equation 14) and systems with the same M could still be subjected to different lower limits on broad-line emission. Thus we need to find the variation range of the luminosity scale Λ.

The lower end of this range can be estimated directly from observations. From the Palomar AGN sample, Elitzur & Ho (2009) find that all broad-line emission disappears at luminosities lower than

$$L_{EH} = 4.7 \times 10^{39} M_7^{2/3} \quad erg\, s^{-1}. \tag{16}$$

Unification then implies that all AGN below this boundary are true type 2 (otherwise there would have been some type 1 counterparts). Since it is based on observations of low-luminosity AGN, this limit is somewhat uncertain, owing to the large uncertainties in determining bolometric luminosities in this regime. The L_{EH} limit conforms to the luminosity constraint of the disc–wind scenario (equation 14), implying a minimum for Λ of

$$\Lambda_{min} \simeq 4.7 \times 10^{39}\, erg\, s^{-1}. \tag{17}$$

This minimum is reached when all three parameters I, r and ϵ have their smallest values. When each has its highest value, the maximum of Λ is obtained. We now estimate one by one the maxima of these three parameters.

3.1 The *I* factor

To estimate the integral I (equation 8), we need the ratio of outflow launch velocity to local Keplerian velocity, $f = v_z(R)/v_K(R)$. The launch velocity is expected to be comparable to the local turbulent velocity (the critical sonic-point condition), thus the quantity needed is the ratio of turbulent velocity to local Keplerian velocity in the disc. The most direct estimate for this ratio comes from high-resolution H$_2$O maser observations. Such observations of the nuclear disc in NGC 3079 show that the velocity dispersion is $\sim$14 km s^{-1} over a small region of strong emission where the Keplerian velocity is 110 km s^{-1} (Kondratko, Greenhill & Moran 2005), suggesting that in the maser region f is probably of the order of $\sim$0.1. Given the lack of information about the turbulent velocity close to the inner disc producing the BLR wind, we assume that the value of f in this region is similar to that derived from the observations further out in the maser region; that is, we make the assumption that at every point in the disc, the turbulent velocity is a fixed fraction, $f \sim 10$ per cent, of the local Keplerian velocity. Then

$$I \simeq 0.1 J, \qquad \text{where} \quad J = \int \eta y^{1/2} dy \tag{18}$$
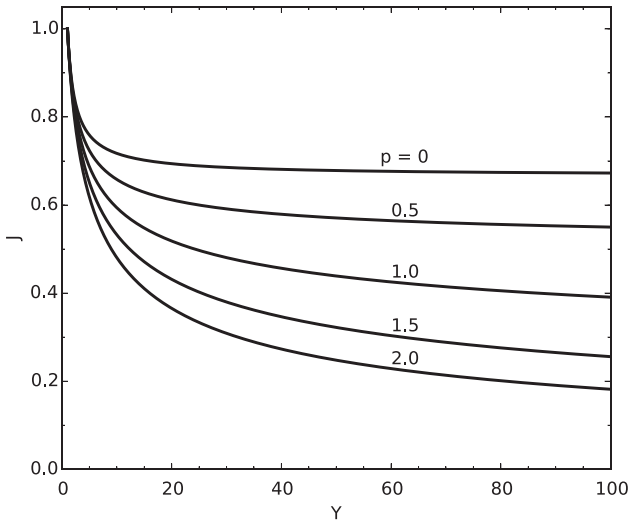
Figure 1. The integral J (equation 18) for power-law radial profiles $\eta \propto y^{-p}$ for various values of p as a function of $Y = R_{out}/R_{in}$, the relative radial thickness; the BLR radial integration range is $1/Y \leq y \leq 1$. Note that $J \to 1$ when $Y \to 1$ because of the normalization of η (equation 7).

and η is the profile of the radial variation of density, properly normalized (equation 7).

Without a detailed model for the BLR dynamics, the functional form of η remains unknown. However, we can still place reasonable limits on the integral J from various power-laws $\eta \propto y^{-p}$, for which the integration is immediate. Fig. 1 shows the variation of J with relative radial thickness Y (ratio of outer-to-inner radius) for representative values of p. The full radial extent of the BLR is expected to be in the range $R_{out}/R_{in} \sim 50$–100, and Fig. 1 shows that J hardly varies with Y in this range. The bulk of the variation comes from the dependence on p; J varies from ~ 0.2 for $p = 2$ to ~ 0.7 for $p = 0$. These values bracket the likely range of J for actual η profiles. Therefore

$$I_{max} \simeq 0.07, \tag{19}$$

a maximum reached for flatter radial density distributions. The figure also shows that the assumption of constant f should not have a marked impact on the outcome – a small radial variation of $f(R)$ could simply be absorbed into the power law.

3.2 The radiative efficiency ϵ

Beginning with the early 1970's, the theory of disc accretion has been investigated in numerous studies. In the standard theory, the mass accretion rate through the disc is constant. Outflows invalidate this assumption, and recent studies by Slone & Netzer (2012) and Laor & Davis (2014) were the first to investigate their effect on the observed disc spectra. We assume that most of the mass outflow takes place at distances that are typical of the BLR, shown by reverberation mapping to be $\sim 10^3$–10^4 GM/c^2, well outside the main continuum producing region, which in standard thin accretion models is of order 50–100 GM/c^2. This allows us to use the standard disc theory to estimate the bolometric luminosity.

For geometrically thin optically thick discs the radiative efficiency ranges from 0.038 for a retrograde disc, to 0.057 for stationary BH to 0.32 for maximally rotating BH with spin parameter of 0.998 (Shakura & Sunyaev 1973). When the effects of radiation capture by the BH are accounted for, ϵ at maximal spinning is reduced to 0.3 (Thorne 1974). Slim accretion discs were suggested to have

smaller efficiency (Wang et al. 2014 and references therein), but this is not yet confirmed by numerical simulations (e.g. Sądowski & Narayan 2015). Recent observational studies provide support for the radiatively efficient solutions for accretion through thin discs. From detailed analysis of spectral properties, Davis & Laor (2011) estimated the values of ϵ for all PG quasars. The majority of the sources are consistent with the theoretical solutions for radiatively efficient accretion through thin discs, with ϵ falling between ~ 6 and 30 per cent. A more detailed analysis of 39 luminous AGN at $z \simeq 1.55$, by Capellupo et al. (2015, 2016), illustrated the very good agreement between the predicted thin disc SED and the observations of all these objects. Given this, we can reasonably take for ϵ the upper limit

$$\epsilon_{max} \simeq 0.3, \tag{20}$$

the radiative efficiency of a maximally spinning accreting BH.

3.3 The r ratio

This is the ratio $r = \dot{M}/\dot{M}_w$ of mass accretion into the BH to mass outflow from the BLR (Section 2.2). Because of the disc outflow, not all the mass that enters the BLR finds its way to the BH. Denote by $\dot{M}_{outer}$ the rate at which mass enters the BLR through its outer disc boundary (the sublimation radius R_d) and by $\gamma = \dot{M}_w/\dot{M}_{outer}$ the fraction of that accreted material lost to the wind. Then the rate of radial inflow from the BLR inner boundary towards the BH is $\dot{M}_{outer}(1 - \gamma)$. As just noted (Section 3.2), the radial mass inflow rate through the disc can be taken as constant inside the BLR inner radius, thus the BH mass accretion rate is $\dot{M} = \dot{M}_{outer}(1 - \gamma)$ and

$$r = \frac{1 - \gamma}{\gamma}. \tag{21}$$

The largest r corresponds to the smallest γ, obtained when the fractional mass carried away by the wind is at minimum. However, the limit $\gamma \to 0$ implies shutting off the outflow altogether, as it carries a smaller and smaller fraction of the accreted mass; that in itself would turn off broad-line emission in the context of the disc–wind scenario assumed here. For any relevance in this context and to have an impact on observable AGN properties, the disc wind must carry some minimal fraction of the accreted mass. Here we assume, somewhat arbitrarily, that for the self-consistency of this scenario this fraction should be at least ~ 10 per cent. This requirement implies that γ must be at least ~ 0.1 in meaningful disc–wind models of the BLR, leading to

$$r_{max} \simeq 9. \tag{22}$$

3.4 The range of Λ

The minimal value of Λ, the proportionality coefficient in the luminosity constraint on broad-line emission (equation 14), was determined directly from observations in equation (17). Determining the maximum requires a theoretical estimate. Combining our estimates for maximal I (equation 19), ϵ (equation 20) and r (equation 22) yields

$$\Lambda_{max} \simeq 3.5 \times 10^{44} \text{ erg s}^{-1}. \tag{23}$$

A large Λ means that observable broad-line emission requires a large bolometric luminosity, increasing the range of luminosities that can lead to true type 2 operation. An AGN is more likely to be a true type 2 if it has I, r and ϵ at the upper end of their

ranges. A larger I implies a flatter density profile (Fig. 1): a larger fraction of the outflow mass resides at larger radii, therefore the same minimal column is accompanied by a larger $\dot{M}_w$, i.e. L. Larger r imply that the outflow carries away a smaller fraction of the mass (equation 21), requiring a larger $\dot{M}_w$, i.e. L, in order to reach the minimal BLR column density. And a larger ϵ means that the mass accretion rate corresponding to the minimal column for a BLR will produce a higher luminosity. At the upper end of Λ, an AGN with a maximally rotating BH ($\epsilon = 0.3$) whose mass is 10^{10} M$_\odot$ will be true type 2 as long as it has $L < 3.5 \times 10^{46}$ erg s^{-1}, a rather high luminosity threshold.

While Λ_{min} was determined from the data, it is instructive to examine its theoretical implications for the minimal values of the parameters I, r and ϵ. From equation (18) and Fig. 1, the smallest I is ~ 0.02, implying that the minimal values of the two other parameters obey $r_{min} \epsilon_{min} \simeq 2 \times 10^{-3}$. The smallest r is obtained from the largest γ, the fraction of the mass carried away by the BLR outflow (Section 3.3). Since the outflow mass applies a back torque on the underlying disc, the amount of material the wind can extract from the disc is limited. In the case of magnetically driven disc winds, an estimate of this upper limit based on the Blandford & Payne (1982) self-similar solution yields $\gamma \lesssim 0.3$ (Emmering, Blandford & Shlosman 1992; Pelletier & Pudritz 1992). This implies $r_{min} \sim 2$ (equation 21) and $\epsilon_{min} \sim 10^{-3}$. Mass extraction by the outflow might reach a higher maximum as a result of other effects, e.g. radiation pressure. Increasing the maximal γ to 50 per cent, so that fully a half of the mass entering the disc at the BLR outer boundary is blown away and only the remaining half is eventually accreted by the BH, yields $r_{min} = 1$ and $\epsilon_{min} \sim 2 \times 10^{-3}$. These estimates for ϵ_{min} are compatible with theoretical expectations for low accretion rates: As $\dot{M}$ decreases below the values assumed in classical accretion-disc solutions (Section 3.2), thermalization times become longer, the solution switches to the advection dominated accretion flow (ADAF) mode and the radiative efficiency decreases to $\sim 10^{-3}$ (for recent reviews, see Narayan 2002; Yuan 2007).

3.5 High-luminosity true type 2 AGN

Fig. 2 summarizes our results, showing in the $L - M$ plane the luminosity boundaries for observable broad emission lines for the two extremes of Λ (equations 17 and 23). Hatching indicates the domain of super-Eddington luminosities. Because of the different M-dependences of L_{min} and L_{Edd}, their contours intersect in the $L - M$ plane at a mass whose value can be determined from equation 15. The lower red boundary, marked 'min Λ', corresponds to the minimal values of I, r and ϵ. As the parameters increase, the boundary moves upwards and when all three reach their maximal values, Λ is the largest and the boundary becomes the upper red curve, marked 'max Λ'. If broad-line emission is properly described by the disc–wind scenario then all AGN below the low boundary are true type 2 and all AGN above the upper boundary are broad-line emitters. We reemphasize that this prediction is an immediate consequence of mass conservation and applies to all disc outflows whether smooth or clumpy and whatever the dynamics model at their foundation.

The lower red boundary corresponds to the luminosity L_{EH} (equation 16). As noted above, this is currently the lowest luminosity observed for any broad-line emitting AGN (Elitzur & Ho 2009). But the disappearance of all broad-line emission below L_{EH} does not imply that it must exist in every object above this limit: sources above the lower red boundary *can* be true type 2, below the upper red boundary they *can* be broad-line emitters, hence in between these boundaries they can be either. An AGN in this intermediate
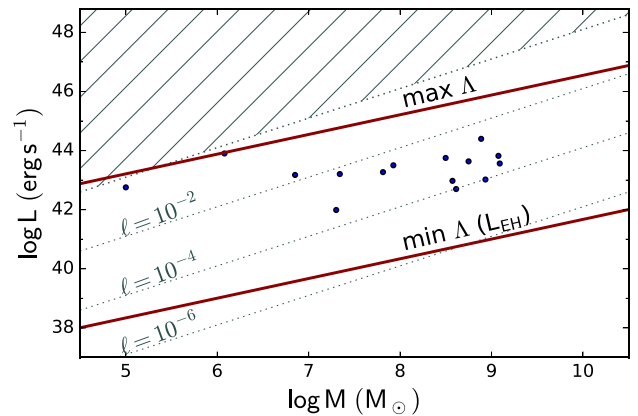
Figure 2. Domains in the $L - M$ plane. The hatched region marks super-Eddington luminosities; also shown are contours (grey dotted lines) for several Eddington ratios $\ell = L/L_{Edd}$, as marked. The two red curves show the low-luminosity boundary for broad-line emission (equation 14) for the minimal and maximal values of Λ (equations 17 and 23), as marked. According to the disc–wind scenario all sources below the low red boundary are true type 2 AGN, all sources above the upper one are broad-line emitters and in between they can be either. Dots are the data from Table 1.

region will display broad-line emission only if its own parameters are such that $L/M_7^{2/3} > \Lambda(I, r, \epsilon)$, otherwise it will be a true type 2. In particular, just below the upper red boundary an AGN could still be a true type 2 if it had a standard thin disc around a maximally spinning BH ($\epsilon = 0.3$) and if its r and I were at the upper end of their ranges. We will refer to objects with $L/M_7^{2/3} < \Lambda(I, r, \epsilon)$ in the $L - M$ domain between the two red boundaries as *high-luminosity true type 2 AGN*. Since the BLR can disappear anywhere below the upper red boundary, type 2 AGN can exist at any Eddington ratio and at luminosities as high as a few 10^{46} erg s^{-1}. Sources that have both high masses and high Eddington ratios will not become true type 2 – the Eddington ratio of a 10^{10} M$_\odot$ AGN on the upper red boundary is only 2.8 per cent. Searches for true type 2 AGN will have higher success rates at lower Eddington ratios because every AGN can be a true type 2 at Eddington ratio below ~ 1 per cent. Similarly, at masses lower than 2.2×10^5 M$_\odot$ every sub-Eddington AGN can be a true type 2.

4 COMPARISON WITH OBSERVATIONS

To determine whether broad lines are missing from the observed spectrum of an AGN, we need to establish the line intensity expected in the source. From the large body of observations, empirical relations have been derived for the dependences of line equivalent widths (EWs) on source luminosity, host galaxy luminosity, the aperture used for the spectroscopic observations, and the signal to noise of the observations. Perhaps the most suitable line in the optical part of the spectrum is Hα, the strongest broad emission line observed from the ground in low redshift AGN. Detailed studies of broad emission lines in low redshift SDSS AGN of low to intermediate luminosity show a large range of 300–600 Å for EW(bHα), the broad Hα EW relative to the intrinsic AGN continuum (Greene & Ho 2005; Stern & Laor 2012a, and references therein). The distribution is very broad and sources with EW(bHα) smaller than 200 Å are quite common. Very high luminosity type 1 AGN tend to show somewhat smaller EW(bHα) (e.g. Capellupo et al. 2015), but the difference may not be statistically significant. Most, perhaps all of these sources are expected to be powered by standard, high

Table 1. Confirmed true type 2 AGN: (1) Source identification; (2) bolometric luminosity; (3) BH mass; (4) Eddington ratio $\ell = L/L_{\rm Edd}$; (5) the largest luminosity and (6) smallest radiative efficiency that would still be consistent with a true type 2 classification for the source (from equations 24 and 25, respectively); (7) references: B – Bianchi et al. (2012); H – Ho et al. (2012); M – Miniutti et al. (2013); P – Pons & Watson (2014); T – Tran, Lyke & Mader (2011); S – Shi et al. (2010); SL – Stern & Laor (2012b).

(1) Source ID	(2) L (erg s^{-1})	(3) M (M$_\odot$)	(4) ℓ	(5) $L_{\rm min\,>}$ (erg s^{-1})	(6) $\epsilon_{\rm m}$ (per cent)	(7) ref
IRAS 01428−0404	9.8E+41	2.0E+07	3.9E−04	5.6E+44	0.3	S,SL
NGC 3147	5.0E+42	4.1E+08	9.7E−05	4.2E+45	0.2	B
J1231+1106	5.7E+42	1.0E+05	4.5E−01	1.6E+43	13.6	H
3XMM 275370	9.5E+42	3.7E+08	2.0E−04	3.9E+45	0.3	P
3XMM 47793	1.1E+43	8.6E+08	9.7E−05	6.8E+45	0.2	P
NGC 3660	1.5E+43	7.1E+06	1.7E−02	2.8E+44	3.3	B
1ES 1927+6054	1.6E+43	2.2E+07	5.8E−03	5.9E+44	2.0	T,SL
3XMM 93640	1.9E+43	6.5E+07	2.3E−03	1.2E+45	1.3	P
3XMM 266125	3.2E+43	8.4E+07	3.0E−03	1.5E+45	1.7	P
3XMM 303293	3.7E+43	1.2E+09	2.4E−04	8.7E+45	0.5	P
3XMM 305003	4.3E+43	5.6E+08	6.1E−04	5.2E+45	0.8	P
3XMM 339379	5.6E+43	3.2E+08	1.4E−03	3.5E+45	1.4	P
3XMM 1780	6.6E+43	1.2E+09	4.4E−04	8.5E+45	0.8	P
GSN 069	8.0E+43	1.2E+06	5.3E−01	8.6E+43	28.5	M
Q2131−427	2.5E+44	7.7E+08	2.6E−03	6.4E+45	2.6	B

efficiency accretion discs (Netzer & Trakhtenbrot 2014). The observational uncertainties on EW(bHα) can be large, especially among low-luminosity AGN where the host galaxy contribution inside the chosen aperture (e.g. the 3 arcsec SDSS fibre) can exceed the AGN contribution, making the subtraction of stellar light quite uncertain. The uncertainties for type 1 LINERs, which may be powered by ADAF, are so large that it is not at all clear whether the typical EW(bHα) distribution of such sources is similar to that observed in the other type 1 AGN. The mean observed value adopted here is EW(bHα) = 500 Å.

According to Stern & Laor (2012a), there is a strong linear correlation between the broad Hα luminosity, $L_{\rm bH\alpha}$, and the AGN bolometric luminosity L, as derived from X-ray observations, and the above mean EW corresponds to $L \simeq 130 L_{\rm bH\alpha}$. Practical lower limits for Hα detection in type 1 AGN can be set at 10 per cent of the expected values, namely, EW(bHα) $\simeq$ 50 Å or $L_{\rm bH\alpha} \simeq L/1300$. Below these limits we classify the source as a true type 2 AGN. Sources with intermediate EW(bHα), of order 50–100 Å, are considered to be intermediate-type AGN. We also note that EW(Hβ) $\simeq 0.2$ EW(Hα) typically, thus our critical EW(bHα) corresponds to EW(bHβ) $\simeq$ 10 Å; this would be a very weak broad line, hard to detect among the numerous broad and narrow lines in the wavelength range 4800–4900 Å centred on Hβ.

It is not our intention to carry out a systematic search of the literature for true type 2 AGN that obey the strict upper limit set here on the broad Hα line. Instead, we focus on a small group where a very detailed, high-quality study has already been carried out to establish the nature of each source as a true type 2 AGN. Table 1 summarizes the properties of such published cases, listing them in order of increasing L. The list is by no means complete but rather based on carefully checked observations known to us. The listed luminosities and BH masses are from the original papers. In the absence of broad lines, the mass estimates are generally based on correlations with bulge properties, which carry a typical error of 0.5 dex (e.g. Läsker et al. 2014). The uncertainty in L depends on the X-ray observations and the conversion between $L(2–10$ keV) and L. The assumption for all sources listed here is that their X-ray

luminosity scales with L the same as in 'typical' type 1 AGN, an assumption that is not directly testable for true type 2s. In this case, the uncertainty on L is about 0.2–0.3 dex. Of the 15 listed sources, the two with the smallest BH masses stand out with their very high Eddington ratios.

The quantities $L_{\rm min\,>}$ and $\epsilon_{\rm m}$, tabulated in columns 5 and 6, respectively, were derived for each object from the disc–wind scenario described above. According this scenario, an AGN transitions into the true type 2 class when its luminosity drops below $\Lambda M_7^{2/3}$ (equation 14). Denote by $L_{\rm min\,>}$ the transition luminosity corresponding to the maximal value of Λ (equation 23)

$$L_{\rm min>} = 3.5 \times 10^{44}\, M_7^{2/3} \ {\rm erg\, s}^{-1}. \tag{24}$$

Listed in column 5, $L_{\rm min\,>}$ would be the location on the upper red boundary in Fig. 2 of an AGN with the same BH mass. Given the uncertainty on the BH mass, the uncertainty on $L_{\rm min\,>}$ is about 0.3 dex. For a given AGN, absence of broad-line emission is compatible with the mass conservation bound if its luminosity L is lower than its $L_{\rm min\,>}$. Since every listed source has $L < L_{\rm min>}$, they all comply with the disc–wind constraint on true type 2 AGN. In most cases, the bound is obeyed by a sufficiently comfortable margin that $L_{\rm min}$ need not be as large as $L_{\rm min\,>}$, implying that Λ need not be at its maximum, i.e. the parameters I, r and ϵ can be smaller than their maximal values, in particular ϵ could be less than 0.3 (equation 20).

The smallest radiative efficiency, $\epsilon_{\rm m}$, that a source could have and still comply with the condition for BLR disappearance is the one that produces $L_{\rm min} = L$ with r and I at their respective maxima. From equation 14, $L_{\rm min} \propto \epsilon^{4/3}$ when r and I are held fixed, therefore

$$\epsilon_{\rm m} = 0.3 \left(\frac{L}{L_{\rm min>}} \right)^{3/4}, \tag{25}$$

the quantity entered in column 6 of Table 1. This is an estimate of the minimal ϵ; the actual radiative efficiency of the source can be anywhere between $\epsilon_{\rm m}$ and 0.3. The uncertainty on $\epsilon_{\rm m}$ depends on the uncertainties on L and M, and is of order 0.4 dex. The derived range of ϵ is reasonably tight for the two objects with the highest Eddington ratios, consistent with thin accretion discs with a spin

parameter larger than 0.7, i.e. close to maximum spinning. For all other sources the range is too wide for a meaningful constraint. Still, it is interesting that they all have ϵ_m below the thin disc minimum of 0.038, consistent with the ADAF discs expected at their low Eddington ratios, which are below ~1 per cent.

Fig. 2 shows the positions of the tabulated sources in the $L - M$ plane. All of them fall below the upper red boundary, in agreement with a true type 2 classification for values of Λ intermediate between its two extremes (equations 17 and 23). The absence of broad-line emission in all of these unobscured sources agrees with the luminosity constraint arising from mass conservation in the disc–wind scenario.

5 SUMMARY AND DISCUSSION

Outflows are widely recognized as an important component of the AGN environment, and magnetically driven winds are plausible candidates for the origin of high-velocity outflows from the inner radii of AGN accretion discs (Peterson 2006; Slone & Netzer 2012, and references therein). Broad-line disappearance at some low AGN luminosity is inherent to the BLR outflow scenario since broad-line emission requires a minimal column density, implying a minimal outflow rate and thus a minimal accretion rate. This result is independent of the detailed wind dynamics, which is still poorly understood. Although a general formulation of the disc outflow from first principles does not yet exist, the luminosity bound formulated here is applicable whatever the details of such future theory might be. Dynamics considerations may only add additional constraints. For example, Nicastro (2000) considered the interplay between radiation- and gas-pressure in disc outflows and found a different bound on the luminosity of broad-line emitting AGN. This model-specific bound, and others like it, can only supplement the mass-conservation bound derived here, which is always applicable.

The fundamental constraint on broad-line emission conveniently splits the problem into its separate elements. The minimal column density $N_{\rm H,min}$ required for broad-line emission is determined purely by atomic processes, independent of any considerations of the BLR detailed structure. The BH and outflow parameters combine to form another characteristic column, $N_{\rm w}$. Mass conservation imposes the limit in equation (9) that involves these two fundamentally different column densities and the additional parameter I, the only quantity with dependence on the wind detailed structure (equation 8). Because $N_{\rm H,min}$ is different for different emission lines, various broad lines could disappear at somewhat different luminosities and produce line ratios that differ from standard broad-line spectra. For example, the main emission region for the Balmer lines is about three times further away than the formation region of C IV1549. The latter also require smaller critical column. Thus a reduction in accretion rate could produce an abnormally large (relative to type 1 AGN) C IV1549/Hα line ratio during the transition stage from type 1 to true type 2.

The resulting limit on luminosity of broad-line emitters (equation 13) is independent of the wind dynamics. The large spread in luminosities of the transition to true type 2 (equations 17 and 23) primarily reflects the large range predicted for the radiative efficiency ϵ, covering the entire range of fast spinning BHs surrounded by thin accretion discs to low-efficiency ADAFs. When operating at the upper end of the range of Λ, an AGN with $M = 10^{10} \, {\rm M}_\odot$ will become a true type 2 when its luminosity drops below 3.5×10^{46} erg s^{-1}, well inside QSO range. Objects with high efficiency are those where the same L is obtained with lower $\dot{M}_{\rm w}$ and hence are more likely to

lose their broad-line emission, especially if the outflow also has a shallow radial density profile. This scenario predicts that true type 2 AGN should show an increased abundance of BH with high spin parameter.

An AGN loses its broad-line emission when $L/L_{\rm min}$ decreases to <1, which can happen at any Eddington ratio (see equation 15 and Fig. 2). The present analysis shows that the AGN sub-pc structure could be controlled by an entirely different luminosity scale, $L_{\rm min} = \Lambda M_7^{2/3}$ (equation 14). The scale factor Λ not only varies among AGN but for a given source it can also vary as it evolves. Does every AGN go through a true type 2 phase? We note that $L \propto \epsilon \dot{M}$ while $L_{\rm min} \propto \epsilon^{4/3}$ when the other properties remain constant. The AGN will lose its BLR as $\dot{M}$ is decreasing only if $L/L_{\rm min} \propto \dot{M}/\epsilon^{1/3}$ drops below unity at some point; that is, the transition to a true type 2 occurs only if $\dot{M}/\epsilon^{1/3}$ decreases with the accretion rate, therefore the issue revolves around the behaviour of this ratio. The fact that true type 2 AGN do exist indicates that this ratio does indeed decrease with $\dot{M}$, at least in some sources. For standard accretion discs, ϵ cannot change on a short (several thousand years) time-scale, since this is basically the BH spin, and the transition to true type 2 follows directly from the drop of $\dot{M}$.

5.1 Toroidal obscuration region

Although our focus here is BLR properties, the disc–wind scenario has similar implications also for the TOR. However, deriving a quantitative estimate for the equivalent of $L_{\rm min}$ (equation 14) for TOR disappearance is more difficult because it brings in the outflow properties of the TOR, whose relation to those of the BLR and the AGN bolometric luminosity L is unknown. A direct comparison of the radial columns through the TOR and BLR can be obtained with the aid of equation (8), which shows that $N_{\rm R} \propto \dot{M}_{\rm w}/I$ for the column through each of these two outflow regions, with the same proportionality coefficient for both. Therefore $N_{\rm R}^{\rm TOR} = N_R^{\rm BLR} \times (\dot{M}_{\rm w}^{\rm TOR}/\dot{M}_{\rm w}^{\rm BLR}) \times (I^{\rm BLR}/I^{\rm TOR})$, with superscripts denoting the respective quantities in each of the two regions. From the definition of I in equation (18) it is straightforward to show that $I^{\rm BLR}/I^{\rm TOR} < 1$, whatever the functional form of the radial density profile η.[2] But the ratio $\dot{M}_{\rm w}^{\rm TOR}/\dot{M}_{\rm w}^{\rm BLR}$ is entirely unknown, and cannot be estimated without a full theoretical model for the disc outflow around AGN. Such a model would have to include all relevant forces, in particular the radiation pressure which can be widely different in the two regions.

Since a calculation of $L_{\rm min}$ is not yet feasible for the TOR, we cannot determine in any given source whether the TOR should disappear before the BLR or the other way round. In principle, there could exist both true type 2 AGN and broad-line emitters with and without dust obscuration. However, the basic fact that the TOR must disappear below some accretion rate is inherent to the disc wind scenario: dust obscuration requires a minimal column density therefore the TOR, too, must disappear at sufficiently low accretion rates and with it the AGN mid-infrared (MIR) emission. That is, dust obscuration of both the central continuum and the broad lines should disappear at some low luminosity and the ratio

---

[2] Because of the normalization of η (equation 7), the integration in equation 18 obeys $\int \eta y^{1/2} {\rm d}y = \bar{y}^{1/2}$, where $\bar{y}$ is the value of y at some point inside the integration range. And because $y \geq 1$ for the TOR while $y \leq 1$ for the BLR, J is >1 for the former and <1 for the latter. This also shows that $J \to 1$ for either region when $Y \to 1$ (cf. Fig. 1).

L_{MIR}/L should decrease when the luminosity drops below a certain, yet undetermined value.

The above predictions are partly supported by the observations. Chiaberge, Capetti & Celotti (1999) find that torus obscuration disappears in low-luminosity ($\lesssim 10^{42}$ erg s^{-1}) FR I radio galaxies, and Maoz et al. (2005) find similar results for LINERs. MIR observations are required to look for torus dust emission in such systems. Some evidence supporting the decline of MIR emission in LINERs comes from recent works by Rosario et al. (2013) and González-Martín et al. (2015). Disappearance of the torus IR emission has been reported also in a number of individual low-luminosity sources (Whysong & Antonucci 2004; Perlman et al. 2007; Müller-Sánchez et al. 2013).

The predicted torus disappearance at low L does not imply that the disc wind is abruptly extinguished, only that its outflow rate is lower than in high-luminosity AGN. When the mass outflow rate drops below these 'standard torus' values, the outflow still provides toroidal obscuration as long as its column exceeds $\sim 10^{21}$ cm^{-2}. Indeed, Maoz et al. (2005) found that some LINERs do have obscuration, but much smaller than 'standard'. Line transmission through a low-obscuration torus might also explain the low polarizations of broad Hα lines observed by Barth, Filippenko & Moran (1999) in some low-luminosity systems.

5.2 Potential alternative explanations

Could there be other explanations for broad-line disappearance? Since broad lines arise from reprocessing of the central continuum, detectable broad emission lines require sufficiently strong ionizing continuum and efficient conversion of this continuum to line radiation. The latter involves the BLR column density, i.e. the matter distribution in the radial direction, and its covering factor, i.e. the angular distribution. Having concentrated on the column density, we now examine the potential role of the two other factors.

5.2.1 Disc SED

We can estimate the influence of different SEDs on observed line EWs using previous studies of large AGN samples. In particular, in sources powered by standard accretion discs, we can examine the possible connection between line EW and the intensity of the 'big blue bump' (BBB), the part of the SED around 1000–3000 Å which is directly observed in many sources and must be related to the shape of the ionizing continuum at wavelengths below 912 Å.

Thin accretion disc models show that, given BH mass and spin, a smaller accretion rate is more noticeable in the short wavelength part of the spectrum and hence affects the Lyman continuum radiation more than the continuum at 4861 Å or 6563 Å, the respective wavelengths of the Hβ and Hα lines. Such variations also affect the intensity of the BBB relative to the longer wavelength continuum. The shape of the SED is also associated with BH mass. Accretion discs around more massive BHs but similar L/L_{Edd} and BH spin are predicted to have weaker BBB and smaller ratios of Lyman continuum to optical luminosity, which would decrease the Balmer line EWs. All predictions regarding disc SEDs are verified by a recent detailed comparison of accretion disc models with the data of 39 AGN (Capellupo et al. 2015, 2016). Here, and in several earlier, somewhat less detailed studies (see Capellupo et al. 2015 for references), the steeper SED and weaker BBB as functions of accretion rate, BH mass and spin are all demonstrated quite

clearly. Given this, one may argue that true type 2 AGN are weak line emitters because of their softer SED, the result of the lower accretion rate. A definitive study of this issue requires comparisons of line EWs in larger samples that cover sources with different luminosity, accretion rate (or L/L_{Edd}) and BH mass, and represent the entire AGN population (which the Capellupo et al. sample did not).

The observational situation regarding broad-line EWs has been studied in great detail under the title 'The Baldwin effect' (Baldwin 1977), the well-known correlation of the EWs of several broad emission lines with continuum luminosity. While clearly observed in several strong UV lines, such as C IV1549 (Risaliti, Salvati & Marconi 2011, and references therein), the hydrogen Balmer lines produce conflicting results. For example, Greene & Ho (2005) provide observational correlations between L(Hα), L(Hβ) and L_{5100} (the 5100 Å luminosity) for sources with $L_{5100} = 10^{42.5}$–10^{45} erg s^{-1}. For the Hβ line this study finds a correlation that can be translated to EW(Hβ) $\propto L_{5100}^{1.13}$, the opposite of what is observed for C IV1549, i.e. an *inverse* Baldwin effect. However, the systematic study by Stern & Laor (2012a), including sources with $L_{5100} = 10^{41.8}$–$10^{45.2}$ erg s^{-1}, shows a ratio of $L_{bH\alpha}/L_{5100}$ that does not vary with the source luminosity. This can be interpreted as EW(bHα) which is independent of luminosity, i.e. no Baldwin effect. As yet another example we use the sample of 135 sources discussed by Netzer et al. (2004). In this case L_{5100} ranges from $10^{43.4}$–$10^{47.5}$ erg s^{-1} and EW(Hβ) varies from about 100–120 Å at the lowest luminosities to 60–70 Å for the most luminous AGN in the Universe, i.e. a very weak Baldwin effect. This sample contains the most massive BHs, yet the range in EW(Hβ), and L/L_{Edd}, is not very different from that in sources where the BH mass, and AGN luminosity, are three orders of magnitude lower. Finally, studies of very large samples, such as SDSS, also show EW(Hβ) $\sim$60–100 Å for $L_{5100} = 10^{43.5}$–$10^{45.5}$ erg s^{-1}, and no correlation between the two (see fig. 7.16 in Netzer 2013).

It is not our intention to discuss the origin of the Baldwin relationship – an area of much confusion, dominated by various selection effects and biases with no clear physical explanation. We simply point out that the observed Balmer line EWs do not change much across a very large range of physical conditions, much larger than that spanned by the 15 sources in Table 1. This is an indication that the changing ionizing continuum of standard thin accretion discs cannot by itself be the origin of the changing line EWs in type 1 AGN. The conclusion is that, much like type 1 AGN, true type 2 AGN can show weak or strong BBB, depending on their other properties. Needless to say, the predictions of the standard accretion disc scenario regarding the ionizing flux cannot be extrapolated in a simple way to the lower efficiency ADAF systems, where the theory is far less understood.

To explain objects that meet the criterion we set for true type 2 AGN (Section 4) purely by SED effects, the number of ionizing photons would have to be reduced by a full factor of 10. However, since all of the sources listed in Table 1 show strong, high-ionization narrow lines, their broad-line deficits could be attributed purely to a change in the SED only if that change had occurred within the past $\sim$1000 yr, the typical recombination time for the narrow-lines region (NLR). A sharp drop in luminosity a few decades ago is a possibility since the NLR cannot disappear on such a short time-scale. However, L/L_{Edd} for several of the sources in question places them in the domain of standard accretion discs, where a factor of 10 reduction in the accretion rate would not produce a similar decrease in EW(bHα). For example, our calculations of disc SEDs for 1ES1927+6054 (see Table 1) using the Slone & Netzer

(2012) code show that an increase in accretion rate by a factor of 10 relative to the one listed in the table, combined with an assumed spin parameter of 0.7 and no change in covering factor, results in an increase by a factor of 2.5 in EW(bHα). This is far below the difference required to explain the big change in EW(bHα) between a 'typical' type 1 source and a true type 2. A several year monitoring of the sources in Table 1 could provide a more decisive answer to this question. Although current data do not provide definitive evidence, it seems unlikely that in each of the Table 1 sources the number of ionizing photons is less than 10 per cent of that in type 1 AGN with similar optical continuum luminosity.

5.2.2 Covering factors

Whatever the AGN properties, the production of detectable broad lines requires part of its sky to be covered by material that captures a sufficient fraction of the ionizing continuum. The Stern & Laor (2012a,b) study of a large SDSS-selected sample of type 1 AGN shows that at low luminosity, most of them actually appear as intermediate types (type 1.x), with a reduced ratio of broad-to-narrow line strength. For the same data, Elitzur et al. (2014) show that the ratio of broad line to bolometric luminosity decreases along the spectral sequence type $1.0 \rightarrow 1.x \rightarrow$ true type 2, indicating a gradual decline in broad-line covering factor as the accretion rate is decreasing. Thus the broad-line disappearance could be attributed to a diminishing covering factor without the need to invoke a changing column density.

Elitzur et al. proposed that this spectral evolution arises naturally if the wind is seeded with clouds that dominate its broad-line emission. Remarkably, the same quantity N_w (equation 9) sets the scale not only for the mass outflow rate but also for the dynamics of cloud motions: the clouds are accelerated against the gravitational pull of the central BH by the ram pressure of the wind in which they are embedded, and the ratio of these opposing forces on a cloud with column density N_H^c is controlled by N_H^c/N_w. While the details of this specific model are beyond the scope of this paper, the direct connection with the wind column density is most relevant to our basic proposal. This model involves the additional assumption of cloud-dominated broad-line emission and thus is not nearly as universal as the current result.

5.2.3 Conclusions

Weakening and disappearing broad emission lines in type 1 AGN can result from a changing disc SED, a drop in BLR covering factor or a decrease in ionized column. All three can be related to a declining accretion rate through the disc and it is difficult to disentangle their effects. Moreover, reflecting the matter angular and radial distributions, respectively, the covering factor and column density may be inherently related to each other. But whatever the other effects, the relation $L > L_{min}$ (equation 13) stands out in its universality as an absolute lower limit for detectable broad-line emission from disc outflows. As noted before, broad-line disappearance below this limit arises directly from mass conservation without any additional assumptions about the wind clumpiness, structure or dynamics, and thus is a fundamental property of the disc–wind scenario. Within this scenario, broad-line disappearance triggered by a decrease of either ionizing continuum or covering factor will only produce true type 2 AGN with luminosity *higher* than L_{min}.

REFERENCES

Antonucci R., 1993, ARA&A, 31, 473
Baldwin J. A., 1977, ApJ, 214, 679
Barth A. J., Filippenko A. V., Moran E. C., 1999, ApJ, 525, 673
Bianchi S. et al., 2012, MNRAS, 426, 3225
Blandford R. D., Payne D. G., 1982, MNRAS, 199, 883
Capellupo D. M., Netzer H., Lira P., Trakhtenbrot B., Mejía-Restrepo J., 2015, MNRAS, 446, 3427
Capellupo D. M., Netzer H., Lira P., Trakhtenbrot B., Mejía-Restrepo J., 2016, MNRAS, submitted
Chiaberge M., Capetti A., Celotti A., 1999, A&A, 349, 77
Davis S. W., Laor A., 2011, ApJ, 728, 98
Elitzur M., 2008, New Astron. Rev., 52, 274
Elitzur M., Ho L. C., 2009, ApJ, 701, L91
Elitzur M., Shlosman I., 2006, ApJ, 648, L101
Elitzur M., Ho L. C., Trump J. R., 2014, MNRAS, 438, 3340
Emmering R. T., Blandford R. D., Shlosman I., 1992, ApJ, 385, 460
González-Martín O. et al., 2015, A&A, 578, A74
Greene J. E., Ho L. C., 2005, ApJ, 630, 122
Ho L. C., Kim M., Terashima Y., 2012, ApJ, 759, L16
Kondratko P. T., Greenhill L. J., Moran J. M., 2005, ApJ, 618, 618
Koshida S. et al., 2014, ApJ, 788, 159
LaMassa S. M. et al., 2015, ApJ, 800, 144
Laor A., 2003, ApJ, 590, 86
Laor A., Davis S. W., 2014, MNRAS, 438, 3024
Läsker R., Ferrarese L., van de Ven G., Shankar F., 2014, ApJ, 780, 70
MacLeod C. L. et al., 2016, MNRAS, 457, 389
Maoz D., Nagar N. M., Falcke H., Wilson A. S., 2005, ApJ, 625, 699
Miniutti G., Saxton R. D., Rodríguez-Pascual P. M., Read A. M., Esquej P., Colless M., Dobbie P., Spolaor M., 2013, MNRAS, 433, 1764
Mor R., Netzer H., 2012, MNRAS, 420, 526
Müller-Sánchez F., Prieto M. A., Mezcua M., Davies R. I., Malkan M. A., Elitzur M., 2013, ApJ, 763, L1
Narayan R., 2002, in Gilfanov M., Sunyeav R., Churazov E., eds, Lighthouses of the Universe: The Most Luminous Celestial Objects and Their Use for Cosmology. Springer, Berlin, p. 405
Nenkova M., Sirocky M. M., Nikutta R., Ivezić Z., Elitzur M., 2008, ApJ, 685, 160
Netzer H., 2013, The Physics and Evolution of Active Galactic Nuclei. Cambridge Univ. Press, Cambridge
Netzer H., Trakhtenbrot B., 2014, MNRAS, 438, 672
Netzer H., Shemmer O., Maiolino R., Oliva E., Croom S., Corbett E., di Fabrizio L., 2004, ApJ, 614, 558
Nicastro F., 2000, ApJ, 530, L65
Panessa F., Bassani L., 2002, A&A, 394, 435
Pelletier G., Pudritz R. E., 1992, ApJ, 394, 117
Perlman E. S. et al., 2007, ApJ, 663, 808
Peterson B. M., 2006, in Alloin D., ed., Lecture Notes in Physics, Vol. 693, Physics of Active Galactic Nuclei at all Scales. Springer-Verlag, Berlin, p. 77
Pons E., Watson M. G., 2014, A&A, 568, A108
Risaliti G., Salvati M., Marconi A., 2011, MNRAS, 411, 2223
Rosario D. J., Burtscher L., Davies R., Genzel R., Lutz D., Tacconi L. J., 2013, ApJ, 778, 94
Shakura N. I., Sunyaev R. A., 1973, A&A, 24, 337
Shi Y., Rieke G. H., Smith P., Rigby J., Hines D., Donley J., Schmidt G., Diamond-Stanic A. M., 2010, ApJ, 714, 115
Slone O., Netzer H., 2012, MNRAS, 426, 656
Stern J., Laor A., 2012a, MNRAS, 423, 600

Stern J., Laor A., 2012b, MNRAS, 426, 2703
Sądowski A., Narayan R., 2015, MNRAS, 454, 2372
Thorne K. S., 1974, ApJ, 191, 507
Tran H. D., 2001, ApJ, 554, L19
Tran H. D., 2003, ApJ, 583, 632
Tran H. D., Lyke J. E., Mader J. A., 2011, ApJ, 726, L21
Wang J.-M., Qiu J., Du P., Ho L. C., 2014, ApJ, 797, 65

Whysong D., Antonucci R., 2004, ApJ, 602, 116
Yuan F., 2007, in Ho L. C., Wang J.-W., eds, ASP Conf. Ser. Vol. 373,
    The Central Engine of Active Galactic Nuclei. Astron. Soc. Pac., San
    Francisco, p. 95

This paper has been typeset from a TEX/LATEX file prepared by the author.